

Preparation and effects of irradiation-induced disorder in PbMo_6S_8 thin films

G. Hertel, H. Adrian, J. Bieger, C. Nölscher, L. Söldner, and G. Saemann-Ischenko
*Physikalisches Institut der Universität Erlangen-Nürnberg, Erwin-Rommel-Strasse 1,
 D-8520 Erlangen, Bundesrepublik Deutschland*

(Received 3 May 1982)

We report the first low-temperature-irradiation experiment of thin films of the Chevrel-phase superconductor PbMo_6S_8 with fast ions (20-MeV sulfur). The films were prepared by dc magnetron sputtering and had superconducting critical temperatures T_c up to 12.85 K (midpoint) with onsets of superconductivity up to 14.7 K. As a function of fluence, T_c , the initial slope of the upper critical field $(dH_{c2}/dT)_{T=T_c}$, the low-temperature resistivity $\rho(16\text{ K})$, and its temperature dependence $\rho(T)$ have been measured. The $H_{c2}(T)$ and ρ data indicate a defect-induced reduction of the electronic density of states at the Fermi level $N(E_F)$. This appears to be responsible for the strong decrease of T_c which drops below 1.2 K at the comparatively very low fluence of 10^{14} cm^{-2} . The T_c decrease is accompanied by a change in the behavior of $\rho(T)$ from metallic with a residual resistance ratio of about two to less than one at a fluence of only $3.9 \times 10^{13}\text{ cm}^{-2}$ where T_c is still 6.32 K. The resistance ratio decreases further with irradiation and is less than 0.5 at $6.5 \times 10^{14}\text{ cm}^{-2}$. We estimate the obtained defect concentrations and propose a simple model which could explain the observed experimental results.

I. INTRODUCTION

Ternary molybdenum chalcogenides with the composition $M_x\text{Mo}_6X_8$ (M =metal or rare earth, X =S,Se,Te) show several interesting physical low-temperature properties and have therefore received widespread interest since their discovery about a decade ago.¹⁻⁴ Since then, almost 100 different so-called Chevrel phases have been found and about two-thirds of them are superconducting above 1.5 K.⁵ The Chevrel structure is a truly ternary structure with nonequivalent lattice sites for the three constituents, and it contains the highest T_c 's of all ternary-structure families with values up to 15.2 K for PbMo_6S_8 .⁶ Most striking, however, are the extremely high critical fields of some of the Chevrel phases, e.g., $H_{c2}(0)$ of $\text{Gd}_{0.2}\text{PbMo}_6\text{S}_8$ is extrapolated to 600 kOe,⁷ and $H'_{c2}=(dH_{c2}/dT)_{T=T_c}$ of LaMo_6Se_8 is 75 kOe/K.⁸

The main structural building blocks are MO_6 octahedra which form the Chevrel phase with three different chalcogenides and many different metals or binary phases are formed without third element at all. Also Mo itself can at least be partially substituted by other transition metals such as Re. This results in the large number of compounds mentioned. Most striking is the large variety of physical properties observed, e.g., high- T_c superconductivity for some compounds such as PbMo_6S_8 and

SnMo_6S_8 , but semiconducting behavior for BaMo_6S_8 or the pseudobinary compounds $\text{Mo}_2\text{Re}_4\text{S}_8$ or magnetic order in part of the rare-earth compound series.⁵ Reasons for this diversity are the different electronic properties of the elements involved, slight variations of the crystal structure, or the occurrence of low-temperature phase transitions.^{9,10} The Chevrel phases can therefore be considered as a very suitable system to study correlations between structural parameters, transport properties, and superconductivity. An important drawback, however, is that in many cases it is difficult to obtain good quality samples because of the brittle nature of these substances and the large differences in the vapor pressures of the constituents.

It is generally agreed upon that the origin of superconductivity in Chevrel phases is due to the Mo d electrons which are strongly localized at the Mo_6 octahedra because the Mo-Mo intracenter distance is about 10–20% smaller than the Mo-Mo intercenter distance. This gives rise to very narrow bands and high needle-shaped peaks in the electronic density of states $N(E)$. This qualitative picture is supported by several band-structure calculations which also show the common feature that there is a gap in $N(E)$ corresponding to 24 electrons per Mo_6 cluster or two electrons per Mo–Mo bond.¹¹⁻¹⁴ Since the properties of these materials depend so

sensitively on the structure and electronic properties of the constituents, it is very interesting to study the consequences of defects. Owing to problems with reproducibility and homogeneity, for most Chevrel phases it appears very difficult to study correlations between physical properties or their dependence on structural and electronic changes by alloying and quenching experiments. However, by means of neutron or ion irradiation the properties of samples can be changed continuously over a wide range and the measurements to establish correlations can be performed with the same sample.

We report the preparation of thin films of the Chevrel phase PbMo_6S_8 and the influence of defects introduced by low-temperature-irradiation experiments using 20-MeV sulfur ions on the superconducting properties, electrical resistivity, and x-ray diffraction data. So far only two irradiation experiments of Chevrel phases are reported in literature. Both experiments used neutrons and sintered samples and were not carried out at low temperature; in one case the irradiation was done at ambient reactor temperature,¹⁵ in the other at low temperature, but the samples were transferred at room temperature to another cryostat for the measurements.¹⁶ Also in both cases only T_c was measured for a few neutron fluences.

II. EXPERIMENT

A. Preparation and properties of PbMo_6S_8 thin films

Thin films were prepared by dc magnetron sputtering in an ultrahigh vacuum (UHV) system which is schematically shown in Fig. 1. A disc of sintered lead molybdenum sulfide was used as a sputtering target to optimize homogeneity and to ensure good electrical as well as thermal contact between target and sputtering cathode. We felt that this technique is more favorable than using MoS_2 partially overlaid by pieces of metal sheets as reported by other authors.¹⁷ The target material was prepared by mixing high-purity molybdenum powder, which had before been reduced for several hours at 1000°C in a H_2 atmosphere, with lead and sulfur in the nominal composition PbMo_6S_8 . The mixture was pressed into pellets and annealed for 24 h at 1050°C in sealed quartz tubes under a helium pressure of about 300 Torr. After regrinding and repressing and a second heat treatment under the same conditions, the pellets had an inductively measured T_c of 14 K (midpoint) and a transition width

(10–90% of the full superconducting signal) of less than 1 K. Variations of composition or annealing conditions did not improve T_c . The sintered lead molybdenum sulfide was pressed into a disc of 3-cm diameter and about 2-mm thickness and mounted to the water-cooled sputtering cathode of the UHV system by a thermally and electrically conducting epoxy resin. The two concentric cobalt samarium magnets enhanced the sputtering rate from about 2 to 10 Å/s. Sapphire substrates were pressed to the sample holder by a stainless-steel mask, which ensured a film geometry suitable for four-probe resistive measurements. The films were 3-mm wide and 12-mm long between the voltage leads. The temperature of the substrates could be varied by filling the substrate holder with fluids of different temperatures, from liquid nitrogen to boiling water. The growth of the films was controlled by a quartz thickness monitor. The initial pressure in the system before the beginning of each sputtering process was always lower than 2×10^{-8} Torr. High-purity 99.9999% argon was used as a sputtering gas. Typical sputtering parameters were an argon pressure of 3×10^{-2} Torr, a voltage of 700 V, and a current of 30 mA. Under these conditions films of about (1–2)- μm thickness were obtained after twenty minutes. The temperature of the sapphire substrates was varied between 77 and 373 K. After the sputtering process the films were annealed for 3 h at 1050°C in sealed quartz tubes to obtain the Chevrel phase. It was found that the substrate temperature during the sputtering must be kept below 300 K; otherwise, the films peel completely off the substrates during the heat treatment.

Without the annealing, the films are amorphous by x-ray analysis and do not become superconducting above 4.2 K. As Fig. 2(a) shows, the resistance of such films increases by a factor of 500 when cooled from room temperature down to 4.2 K. From Fig. 2(b), where the logarithm of the resistivity is plotted versus $T^{-1/4}$, follows that the temperature dependence can be well fitted $\rho(T) \sim \exp(T^{-1/4})$. This is indicative of hopping conductivity. A possible explanation could be that fragments of the Mo_6S_8 clusters rather than single atoms are sputtered from the sintered Chevrel phase sputtering target.

After the heat treatment the best films had resistively measured T_c 's up to 12.85 K (midpoint), which is comparable with the highest values ever published for PbMo_6S_8 thin films, and a transition width of about 0.7 K. The onset of the resistive transition of good samples was higher than 14 K and in some cases as high as 14.7 K. In fields up to

60 kOe all films showed a linear $H_{c2}(T)$ behavior. The films with the highest T_c 's had an initial slope $H'_{c2} = (dH_{c2}/dT)_{T=T_c}$ of only 35 kOe/K. Neglecting effects of paramagnetic limiting, this yields an extrapolated critical field at $T=0$ of about 310 kOe which is almost a factor of 2 below what is obtained with sintered bulk samples. The low-temperature normal-state resistivity varied from 250 to 700

$\mu\Omega$ cm and the room-temperature resistivity varied from 400 to 1200 $\mu\Omega$ cm. This strong scatter is probably due to microcracks in the films which develop during the heat treatment either because of the change in density when the Chevrel phase is formed or different thermal expansion coefficients of film and substrate. Although no cracks are visible, microcracks connected with the same strong

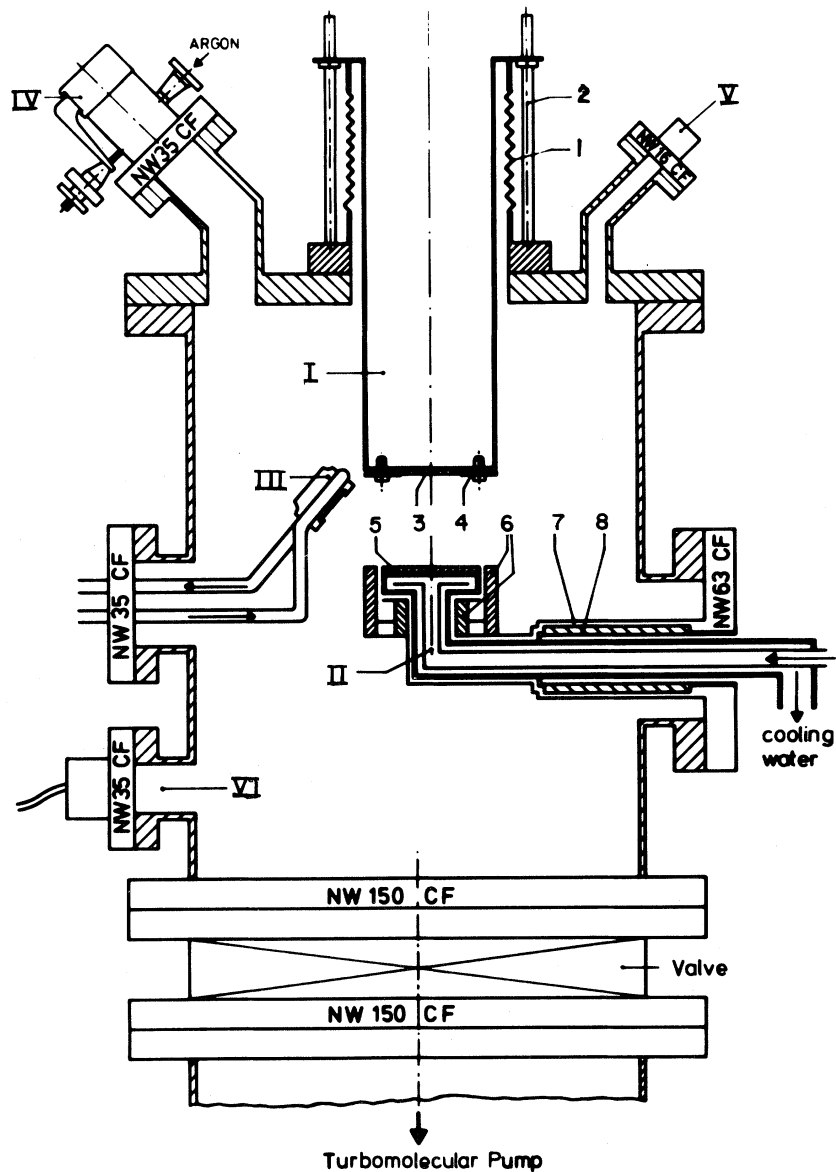


FIG. 1. UHV chamber for dc magnetron sputtering. I, substrate holder (1, bellow; 2, adjustment rods; 3, sapphire substrate; 4, stainless-steel mask); II, sputtering cathode (5, sputtering target; 6, concentric Sm-Co permanent magnets; 7, grounded shield; 8, ceramic high-voltage feedthrough); III, quartz thickness monitor; IV, throttle valve for argon inlet; V, thermocouple vacuum gauge; VI, ion vacuum gauge.

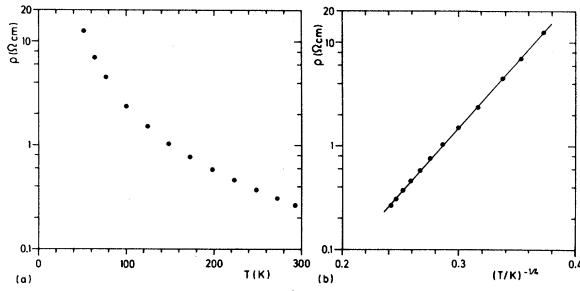


FIG. 2. (a) Temperature dependence of the electrical resistivity of a film sputtered from a sintered PbMo_6S_8 target onto a sapphire substrate held at room temperature before heat treatment. Note the logarithmic resistivity scale. (b) Same as in (a), but plotted vs $T^{-1/4}$.

variation of the electrical resistivity have been observed for PbMo_6S_8 single crystals.¹⁸ Therefore, the measured values given can only be considered as an upper limit for the true resistivity of the Chevrel phase. The temperature dependence of the resistivity of a representative selection of films, normalized to the room-temperature value, is shown in Fig. 3. From a comparison with data published for single crystals we conclude that the positive curvatures in the low-temperature range up to about 50 K might be due to impurity phases. From this we conclude that high resistance ratios are not necessarily an indication of good PbMo_6S_8 films. Figure 4, which contains the T_c and resistance ratio data of all films prepared, shows that the resistance ratio of the good samples ($T_c > 12$ K) can vary between 1.4 and 1.9. However, the data of Fig. 4 also show that there exists a trend, though not a close correlation, where high T_c is accompanied by a comparatively high resistance ratio.

B. Analysis of structure and stoichiometry

The Chevrel phase structure of the reacted films was established by x-ray diffraction using $\text{Cu K}\alpha_1$

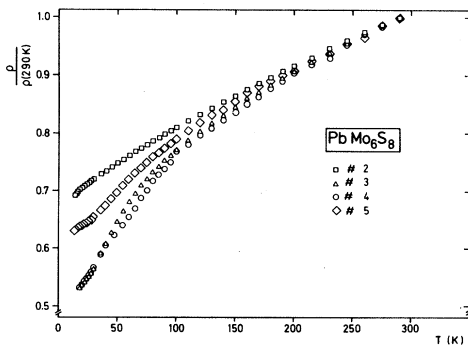


FIG. 3. Typical temperature dependences of the electrical resistivity of PbMo_6S_8 thin films.

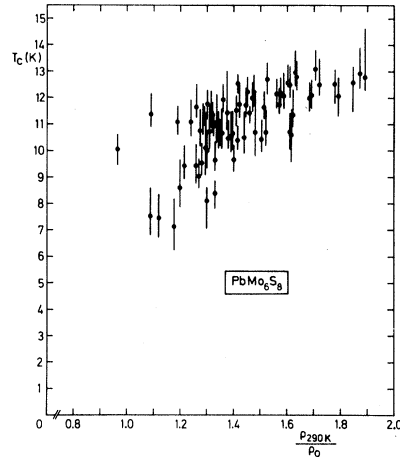


FIG. 4. Variation of T_c vs residual resistance ratio for PbMo_6S_8 thin films. The bars indicate the transition width defined by 10 to 90% of the normal-state resistivity.

radiation in Seemann-Bohlin geometry. A typical diffraction spectrum is shown in Fig. 5. From this we find hexagonal lattice parameters $a = 9.21 \text{ \AA}$ and $c = 11.46 \text{ \AA}$ in agreement with values published for bulk material.¹⁹ For most samples the x-ray data showed a small amount of free molybdenum estimated to be less than 5%, and in some cases traces of Mo_2S_3 were found. Few films were pure Chevrel phase judging from the x-ray data. The thickness and the relative compositions of the sputtered films were determined by elastic backscattering of 12.2-MeV α particles. Figure 6 shows the relevant part of a typical spectrum of backscattered α particles. The strong variation of the sulfur signal originates from the energy dependence of the scattering cross section which was therefore determined in an independent experiment. For the films investigated, which had T_c 's between 10.9 and 12.75 K, variations of the lead content between 0.76 and 0.86 and of the sulfur content between 6.3 and 7.6 normalized to Mo_6 were determined. This means the samples contain excess molybdenum compared to the usual stoichiometry PbMo_6S_8 in agreement with the x-ray data. Nevertheless, this nominal formula will be used throughout the paper to address the films. As for the backscattering data and T_c 's, no convincing correlation could be detected. The attempt to increase the lead content of the sputtered films by adding small amounts of lead in the quartz tubes during annealing resulted in very high resistance ratios, but did not influence T_c . The resistance behavior appeared to be modified due to a lead overlayer on the films, not by an actual change of

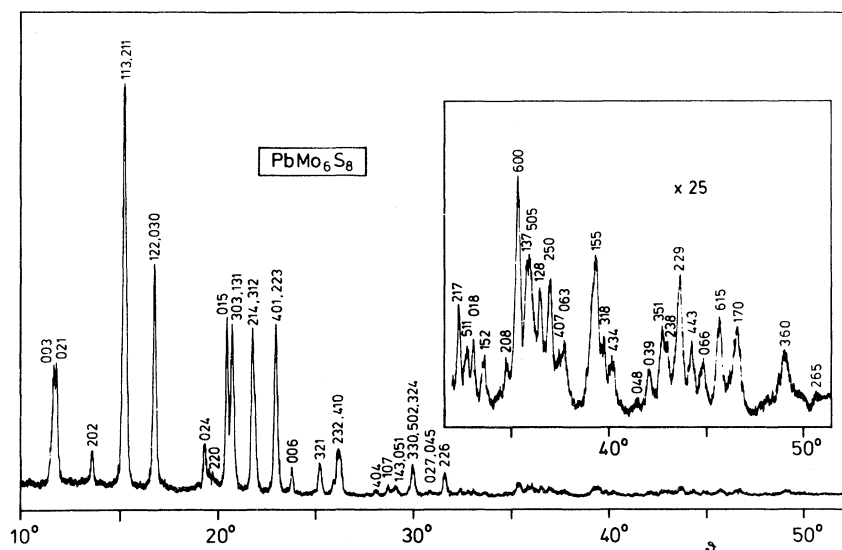


FIG. 5. X-ray diffraction pattern of a Chevrel phase PbMo_6S_8 thin film taken with $\text{CuK}\alpha$ radiation at room temperature. Hexagonal indices are used to identify the lines.

the Chevrel phase. The thickness of the films usually controlled by a quartz monitor was verified by the backscattering experiments to be between 0.5 and 2.5 μm .

C. Low-temperature ion irradiation experiment

For the irradiation experiments, films with T_c 's between 12.3 and 12.7 K and a thickness between 1 and 2 μm were selected. The experiments were carried out at the low-temperature-irradiation facility of the Erlangen Van de Graaf Tandem accelerator using 20-MeV sulfur ions. The focus of the ion beam was formed into a vertical ellipse by a quadrupole magnet and in the horizontal direction swept electrostatically over the length of the films by a triangular shaped voltage at a rate of about 200 cps. The mean range of the projectiles in PbMo_6S_8 is about 6 μm , much larger than the film thickness.

Therefore, no projectiles were implanted in the film and homogeneous damage was achieved. During irradiation the sample temperature was below 20 K; for measurements between irradiations the lowest obtainable temperature was 1.2 K. The cryostat insert could be lifted to locate the sample holder in the center of a 6-T NbTi superconducting solenoid. Further details of the facility are given in Ref. 20. For annealing studies the temperature of the sample holder can be raised quickly and controlled up to 300 K.

III. RESULTS

A. Superconducting critical temperature

The superconducting critical temperature decreases rapidly with irradiation fluence as shown in Fig. 7. At a fluence of 10^{14} cm^{-2} , T_c has dropped below our experimental temperature limit of 1.2 K. The error bars in Fig. 7 show representatively for one sample the 10 and 90% points of the resistive transition. It can be seen that the width of the transition remains approximately constant and that its asymmetry increases. In a wide fluence range the T_c decrease is roughly linear and no indications for saturation effects, as we usually found with A15 compounds, are observed.²¹ It was checked that T_c does not reappear with further irradiation up to a fluence of $6.5 \times 10^{14} \text{ cm}^{-2}$. The extreme sensitivity of T_c of PbMo_6S_8 to irradiation is evident from Fig. 8, where the T_c 's of PbMo_6S_8 and the A15 compound V_3Si normalized to their values before irradiation are plotted versus a logarithmic fluence scale.

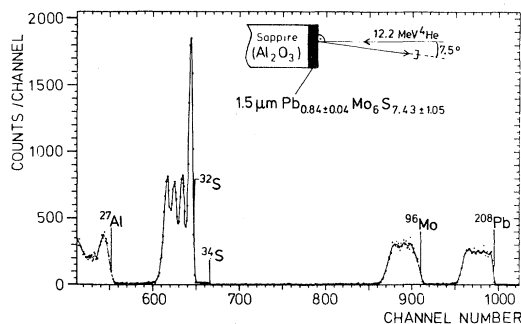


FIG. 6. Relevant part of a typical backscattering spectrum using 12.2-MeV α particles.

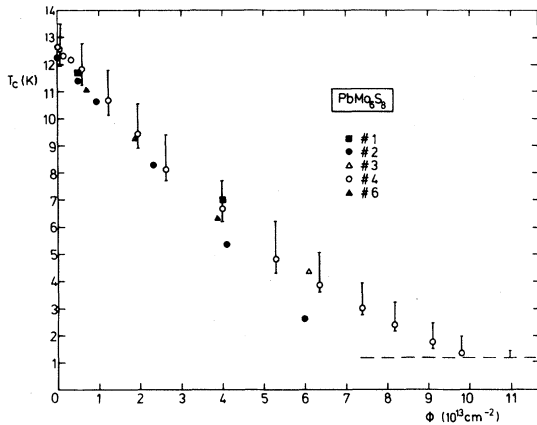


FIG. 7. T_c of PbMo_6S_8 vs fluence of 20-MeV sulfur ions. The bars are representative of the resistive transition width. The dashed line indicates the experimental temperature limit of 1.2 K.

The results shown were obtained under identical experimental conditions. In order to achieve a comparable reduction in T_c , the A15 compound requires fluences which are about a factor of 20 higher. It is worthwhile to mention also that the properties of the ternary rhodium borides exhibit a dependence on irradiation defects very similar to high- T_c A15 compounds.²² Therefore, the behavior of PbMo_6S_8 appears to be quite unique. Annealing up to room temperature has only a slight effect on T_c which further decreases about 0.2 K. The strong T_c depression of Chevrel phases with irradiation was already known from the neutron experiments, although they found a difference in fluence of about a factor of 4 compared to the A15's. However, no in-

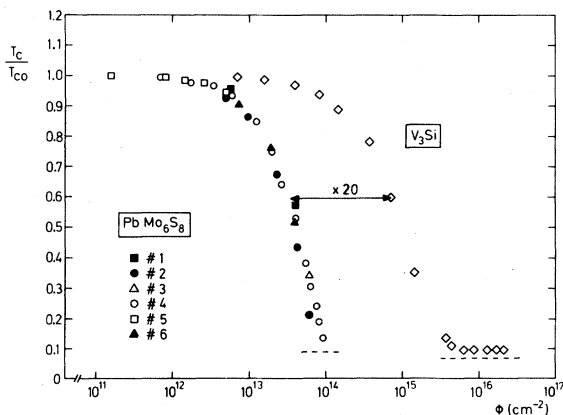


FIG. 8. T_c of the Chevrel phase superconductors PbMo_6S_8 and the A15 superconductor V_3Si normalized to the values before irradiation and plotted vs fluence of 20-MeV sulfur ions. Note that the two compounds require fluences which differ by a factor of 20 for comparable T_c depressions.

formation at all is currently available on any of the following properties.

B. Initial slope of the upper critical field near T_c

The resistive superconducting transitions of the films were also measured in constant external fields up to 60 kOe. Except for the undamaged films, we always observed a low-field anomaly in the $H_{c2}(T)$ curves. In order to calculate $(dH_{c2}/dT)_{T=T_c}$, the initial slope of $H_{c2}(T)$ near T_c , we therefore only used the data taken between 20 and 60 kOe, which always fell very well on a straight line. The results of these measurements are plotted in Fig. 9 versus T_c , which was reduced by irradiation. From the surprisingly low $(dH_{c2}/dT)_{T=T_c}$ of 35 kOe/K of the undamaged films, we calculate the Ginzburg-Landau coherence length $\xi_0 = 33 \text{ \AA}$. After introducing very few lattice defects by irradiation (fluence of less than 10^{13} cm^{-2}) reducing T_c about 1 K, $(dH_{c2}/dT)_{T=T_c}$ is increased by almost a factor of 2 to about 65 kOe/K. We estimate the defect concentration (see Sec. IV B) necessary to raise $(dH_{c2}/dT)_{T=T_c}$ to 60 kOe/K, corresponding to $T_c = 11 \text{ K}$, to less than 2×10^{-3} . From this we calculate a mean distance between irradiation-induced defects of about 20 \AA . In the fluence region considered, the low-temperature resistivity $\rho(16 \text{ K})$ is increased about 40%. Assuming identical scattering cross sections for all kinds of defects, we calculate a mean distance between defects in the undamaged films of about 15 \AA . In order to calculate the

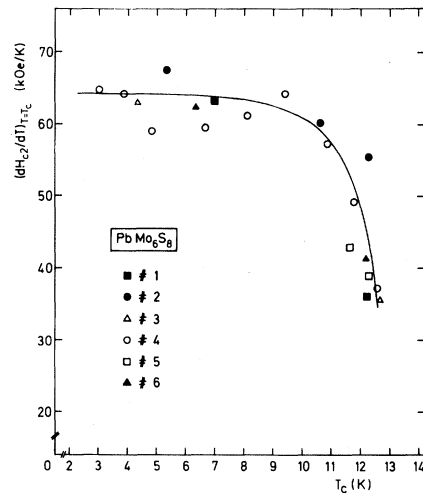


FIG. 9. Initial slope of the upper critical field near T_c as function of T_c which was varied by irradiation. The line was drawn to emphasize the overall trend.

mean free path of the conduction electrons, the scattering cross sections of the defects for electrons is needed. If we assume that a defect causes a distortion of the lattice within a sphere with the radius of the rhombohedral lattice parameter $a_0 \approx 6.5 \text{ \AA}$, we obtain an electronic mean free path l_0 for the undamaged films of about 27 \AA . Therefore, PbMo_6S_8 can be marginally described in the dirty limit. Although several uncertainties enter the outlined estimate of l_0 , this is an independent possibility which does not use the absolute value of the electrical resistivity, a quantity at least questionable for most Chevrel phase materials. Woollam and Alterovitz²³ investigated sputtered PbMo_6S_8 films with $T_c = 11.5 \text{ K}$ and $(dH_{c2}/dT)_{T=T_c} = 60 \text{ kOe/K}$. From our data we conclude that their films have a slightly higher defect concentration which is in agreement with their estimate of $l_0 = 23 \text{ \AA}$. The strong variation of T_c and $(dH_{c2}/dT)_{T=T_c}$ with defect concentration displayed in Fig. 9 appears to be the origin of the wide spread of experimental data reported in literature. For sintered bulk PbMo_6S_8 one usually finds $(dH_{c2}/dT)_{T=T_c}$ between 50 and 60 kOe/K.

C. Electrical Resistivity

The low-temperature electrical resistivity $\rho(16 \text{ K})$ shows a complex behavior upon irradiation which is displayed in Fig. 10. Note that the fluence axis is almost 1 order of magnitude larger than in Fig. 7. For $\phi \geq 10^{14} \text{ cm}^{-2}$, which is the fluence region where T_c drops below 1.2 K, $\rho(16 \text{ K})$ increases by a factor of 4 to 5 over its initial value. This is very similar to the behavior usually found for A15 compounds, except for the much smaller fluences required. However, the occurrence of a maximum

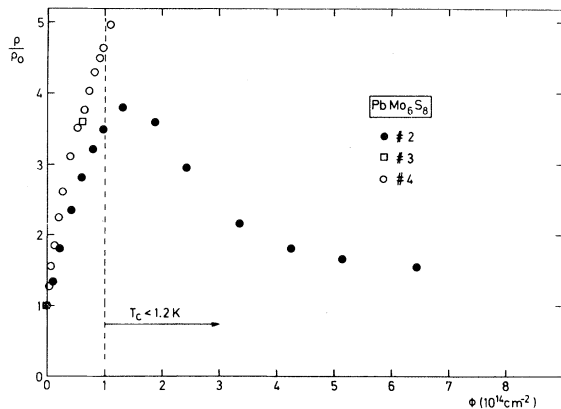


FIG. 10. Low-temperature resistivity $\rho(16 \text{ K})$ normalized to the value before irradiation vs fluence of 20-MeV sulfur ions

and the decrease of $\rho(16 \text{ K})$ at high fluences were unexpected. Owing to the mentioned scatter in ρ only normalized variations are meaningful. As the change in resistivity by irradiation is supposed to be the same for all samples, the differences in the normalized $\rho(16 \text{ K})$ vs ϕ curves can be explained by different initial resistivities. This can also be seen in Fig. 11, where the normalized $\rho(16 \text{ K})$ is plotted versus T_c , which exhibits a linear correlation between these two quantities. Extrapolations of the straight lines intersect the T_c axis at approximately the same point (17.02 and 17.67 K) and show clearly that they only differ by a constant factor due to different normalization. From this one might speculate that clean ideally ordered PbMo_6S_8 would have a T_c as high as 17 K, if it could be prepared. The extrapolation to T_c equal to zero intersects the resistance axis at a value which roughly corresponds to the maximum in $\rho(16 \text{ K})$.

Also, the temperature dependence of ρ measured after irradiation and annealing at 290 K is quite unusual compared to the results obtained for other irradiation-sensitive high- T_c compounds like the A15's or rhodium borides. Generally these materials develop either a temperature coefficient of ρ near zero (Nb_3Al) or a minimum in $\rho(T)$ (V_3Si , ErRh_4B_4) or a small negative temperature coefficient with the low-temperature value of ρ typically a few percent above the room-temperature value (Nb_3Ge , Nb_3Sn , LuRh_4B_4). Furthermore, this well-known behavior is found after fluences on the order of $2 \times 10^{15} \text{ cm}^{-2}$ 20-MeV sulphur ions or $2 \times 10^{17} \text{ cm}^{-2}$ 1.8- or 2-MeV α particles where the samples have been shown to be either x-ray amorphous or can be estimated to be at least highly disordered. In

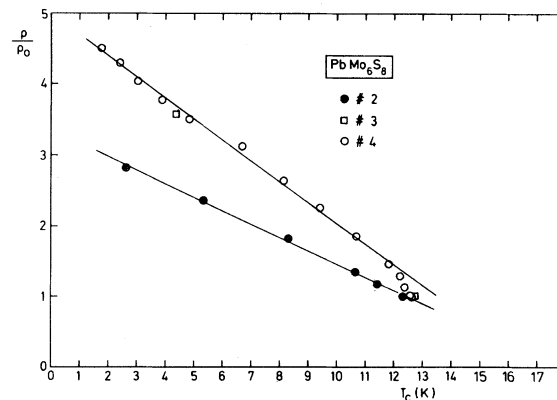


FIG. 11. Low-temperature resistivity $\rho(16 \text{ K})$ normalized to the value before irradiation as function of T_c which was varied by irradiation. The different slopes of the straight lines could be an artifact of the normalization due to different initial defect concentrations.

the case of Nb_3Ge , the high fluence data of the low-temperature resistivity and T_c versus fluence and $\rho(T)$ are very similar to the irradiation behavior of cold condensed amorphous $\text{Nb}_{75}\text{Ge}_{25}$.^{21,24} Therefore, for these compounds it is reasonable to apply theories which have been proposed to explain $\rho(T)$ of amorphous metals, e.g., the extended Ziman theory or phonon-assisted conductivity. The completely different $\rho(T)$ behavior of disordered Chevrel phases is shown in Fig. 12. The curves have been measured after low-temperature irradiation and subsequent annealing at room temperature. For comparison typical $\rho(T)$ curves of unirradiated films are included. Presumably due to the brittleness of the Chevrel phase, the resistance of most films changed during the experiment once or twice abruptly which we believe is caused by the occurrence of additional cracks. Therefore, in Fig. 12 $\rho(T)$ of each film is normalized with the new value $\rho(290\text{ K})$ obtained after irradiation and annealing at room temperature. Two of the samples showed jumps in the resistivity while the $\rho(T)$ data were taken and their estimated behavior is therefore only indicated by the two full lines in Fig. 12. It is evident that the character of $\rho(T)$ changes drastically after irradiation with very small fluences. For in-

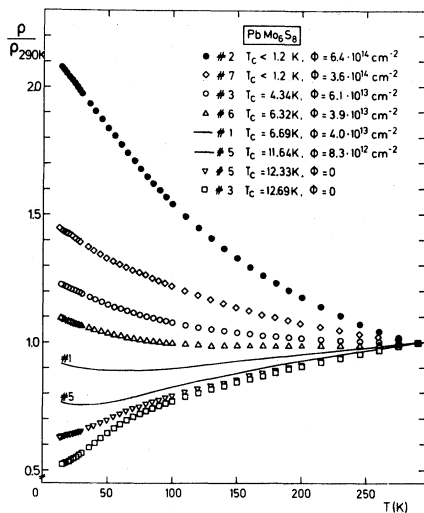


FIG. 12. Temperature dependence of the resistivity measured after irradiation with different fluences at low temperature and annealing at 290 K. The ρ data are normalized to $\rho(290\text{ K})$ in order to stress the temperature dependence. Two samples showed small resistance jumps during the measurements which are presumably due to additional cracks in the films and their estimated behavior is indicated by the full lines. For comparison $\rho(T)/\rho(290\text{ K})$ of two films before irradiation is also shown.

stance, the resistance ratio $\rho(290\text{ K})/\rho(16\text{ K})$ of sample 3 is changed from almost 2 before irradiation to 0.9 after a fluence of just $3.9 \times 10^{13}\text{ cm}^{-2}$ which reduced T_c from 12.69 to 6.32 K. For this fluence we estimate a concentration of displaced atoms (see Sec. IV B) of about 8×10^{-3} . With further irradiation $\rho(16\text{ K})/\rho(290\text{ K})$ continues to increase and reaches a value of almost 2.1 after a fluence of $6.4 \times 10^{14}\text{ cm}^{-2}$. As the resistivity has a very large negative temperature coefficient at comparatively low degrees of disorder, it certainly must be caused by some mechanisms different from those proposed for highly disordered metals. Figure 12 also shows that the shape of $\rho(T)$ of different PbMo_6S_8 samples can vary significantly depending on the concentration and also presumably on the type of defects present.

It is important to point out that only if $\rho(T)$ of each sample is normalized to its room-temperature resistivity after irradiation is the clear fluence dependence of Fig. 12 obtained with the curves lying above each other with increasing fluence. Contrary to A15 compounds, for example, without this normalization $\rho(T)$ curves of samples irradiated with intermediate fluences lie above $\rho(T)$ curves of samples with high fluences or intersect them. In order to clarify the complex resistance behavior of PbMo_6S_8 upon irradiation and annealing, Fig. 13 shows a compilation of all resistance data of two samples which obviously did not change their geometry relevant to electrical resistivity by additional cracks during the whole experiment. For both samples the data have only been normalized once by dividing by the resistance at 290 K before irradiation to eliminate different geometry factors. Figure 13 shows that contrary to T_c there are quite large annealing effects in $\rho(16\text{ K})$ which always lead to an increase of $\rho(16\text{ K})$, independent of whether the irradiation was terminated at a fluence before or after the maximum in the $\rho(\phi)$ curve.

IV. DISCUSSION

A. Superconducting properties

As already mentioned, the band-structure calculations of Chevrel phase compounds show many narrow and high peaks in the electronic density of states $N(E)$ originating from the Mo d electrons strongly localized at the Mo_6 octahedra. In the case of PbMo_6S_8 , the Fermi energy is situated in a peak of $N(E)$ and it is generally agreed that the resulting

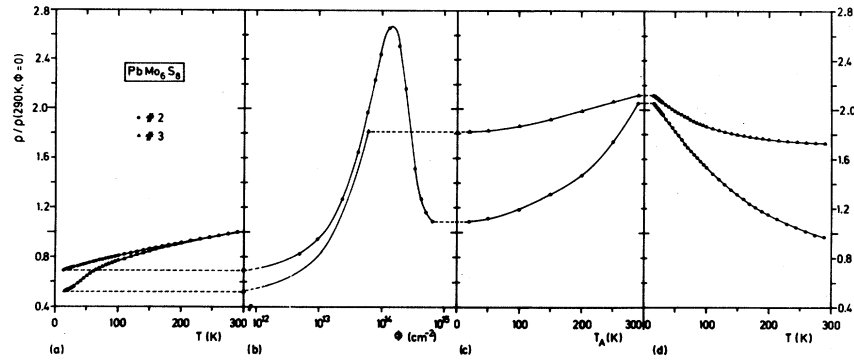


Fig. 13. In order to clarify the complex behavior of the electrical resistivity, a compilation of the resistance data of two samples is shown. Different geometry factors are eliminated by normalization to the value taken at 290 K before irradiation. (a) Temperature dependence of the resistivity before irradiation. (b) Low-temperature resistivity $\rho(16\text{ K})$ vs logarithm of irradiation fluence. (c) Low-temperature resistivity $\rho(16\text{ K})$ vs annealing temperature. (d) Temperature dependence of the resistivity after irradiation and annealing 290 K. Note that sample 3, which has the higher resistivity, was irradiated with a fluence about 1 order of magnitude smaller than sample 2.

rather high value of $N(E_F)$ is an important reason for the relatively high T_c . Further, it has been shown that there appears to be a linear correlation between the electron-phonon coupling parameter λ and the bare density of states at the Fermi energy $N(E_F)$. For this analysis λ was calculated from T_c using McMillan's equation

$$k_B T_c = \frac{\hbar \langle \omega \rangle}{1.2} \exp \left[- \frac{1.04(1+\lambda)}{\lambda - \mu^*(1+0.62\lambda)} \right], \quad (1)$$

with $\mu^* = 0.11$ and $\hbar \langle \omega \rangle = 12\text{ meV}$ for all compounds. The dressed density of states $N^*(E_F)$ was calculated from specific-heat data.²⁵ In order to analyze whether a change of $N(E_F)$ due to defects might be responsible for the observed T_c depression, we used a similar approach: Starting with the assumption $\lambda \sim N(E_F)$ and using in the dirty limit $N^*(E_F) \sim H'_{c2}/\rho$, where $H'_{c2} = (dH_{c2}/dT)_{T=T_c}$ and ρ are taken from the experiment, to calculate changes in $N^*(E_F) = (1+\lambda)N(E_F)$, we obtain the following expression for λ :

$$\lambda(\phi) = -\frac{1}{2} + \left[\lambda_0(1+\lambda_0) \frac{H'_{c2}/\rho(\phi)}{H'_{c2}/\rho(\phi=0)} + \frac{1}{4} \right]^{1/2}, \quad (2)$$

where λ_0 is the value of λ before irradiation.

This equation can also be considered to give λ as a function of H'_{c2}/ρ normalized to its value before irradiation. From λ , again T_c is calculated using McMillan's equation. This finally gives a theoretical correlation between H'_{c2}/ρ and T_c based on the

outlined model which can be compared with the experimental results. From the good agreement shown in Fig. 14 we conclude that a decrease of the density of states is the main reason for the observed defect-induced T_c degradation. However, this line of reasoning is not necessarily conclusive, since one could argue about the validity for Chevrel phases of most of the relations used. This begins with the McMillan equation which has been derived for superconductors with niobium-type Eliashberg functions from which PbMo_6S_8 certainly differs significantly. Also the strong variation of $N(E)$ near E_F could have a considerable effect on T_c not accounted for in McMillan's equation. Another problem is that H'_{c2}/ρ can only be used as a measure for $N^*(E_F)$ if the same electronic band is responsible for the normal-state resistivity as well as superconductivity. An experimental indication that this indeed

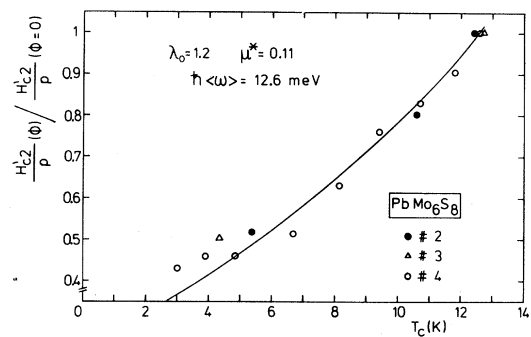


FIG. 14. Full line represents the calculated correlation between H'_{c2}/ρ and T_c as obtained under the assumption outlined in the text. The data points are from the experiment.

might be true in the case of PbMo_6S_8 is the fact that T_c and ρ change on the same fluence scale and both show this extraordinary sensitivity upon irradiation.

One also has to consider changes of the phonon spectrum due to defects to be of importance for the decrease of T_c . It is conceivable that already very small concentrations of displaced atoms which might be located in the channels of the structure could lead to a considerable hardening especially of the external vibrations. But from tunneling experiments and isotope-effect measurements it has been concluded that the internal modes are also important for superconductivity and these should remain essentially unchanged at least for undamaged clusters.²⁶ Therefore, neither the extreme sensitivity of T_c nor especially that of ρ could be explained by a change of the phonon spectrum. A further possibility for the T_c decrease, the degradation of the electron-phonon coupling due to defects, cannot be ruled out. But also in this case the strong sensitivity to defects of T_c as well as $\rho(16\text{ K})$ and $\rho(T)$ appears to be accidental.

Summarizing this section, the observed behavior of T_c , H_{c2} , and $\rho(16\text{ K})$ is consistent with a decrease of $N(E_F)$ due to defects. This and the $\rho(16\text{ K})$ and $\rho(T)$ data could be most naturally explained by a shift of the Fermi level as discussed in the following section.

B. Irradiation-induced lattice defects

The Chevrel structure is comparatively open. Owing to the arrangement of the Mo_6S_8 building blocks, the structure contains orthogonal channels with the Pb atoms located at the intersections. In order to estimate the irradiation-induced defect concentrations after the low fluences applied, it is certainly reasonable to neglect displacements of atoms which cancel an already existing defect. It is assumed that displaced atoms are situated in the channels. Therefore, in the case of Chevrel phases, especially at low fluences, the situation appears to be much simpler than in the case of dense-packed ordered compounds like $A15$'s.

An important quantity necessary to calculate defect concentrations is the mean displacement energy T_d which must be transferred to a target atom to displace it permanently from its lattice site. Since for Chevrel phases no experimental displacement energies are known, we had to use values partly estimated from the corresponding elements. In order to obtain an upper limit for the defect concentra-

tion, we used rather low values for T_d which nevertheless could be a factor of 2 wrong in both directions. As shown in Table I we used a mean displacement energy for lead atoms of 10 eV, considerably less than the value of 25 eV of metallic lead. The Mo_6 octahedra can be considered as parts of bcc molybdenum metal with each atom having half the number of covalent bonds. Therefore, a mean displacement energy of 40 eV compared to 60 eV of the element was taken. The sulfur atoms are situated at the corners of a S_8 cube, and the bonding to the Mo_6 octahedra has ionic character. Since the sulfur atoms form the mentioned open channels, very small energy transfers should be sufficient to displace them. Consequently we used a displacement energy of only 5 eV. A comparison with pure sulfur is not possible, because there are no experimental data, and would probably be meaningless anyway. Furthermore, in Table I the maximum transferred energy T_{max} and the mean transferred energy T are given. From these values for the three different kinds of target atoms we calculated an average displacement energy T_d and an average transferred energy T weighted with the relative concentrations and Rutherford displacement cross sections. Assuming that half of the energy transferred actually leads to the displacement of atoms, whereas the other half is dissipated in electronic excitations and lattice vibrations, we find a mean number of 6.5 displaced atoms per primary knock on atom. The weighted average of the displacement cross sections is $\bar{\sigma}_d = 3.34 \times 10^{-18} \text{ cm}^2$. This gives a mean free path of the 20-MeV sulfur ions as

$$\lambda_d = (n\bar{\sigma}_d)^{-1} = 0.56 \times 10^{-6}, \quad (3)$$

in units of cm, where n is the concentration of target atoms.

From this follows that a fluence of one sulfur ion per cm^2 corresponds to 2.5×10^{-16} displacements per atom (dpa). Therefore, at a fluence of 10^{14} cm^{-2} where T_c drops below 1.2 K, only a fraction

TABLE I. Maximum transferred energy T_{max} , mean transferred energy T , and mean displacement energy T_d for the three different kinds of target atoms Pb, Mo, and S in case of irradiation with 20-MeV sulfur ions. For comparison the displacement energies of Pb and Mo in the pure elements are also given.

Atom	T_{max} (MeV)	T (eV)	T_d (eV)	$T_{d,\text{element}}$ (eV)
Pb	9.3	137	10	25
Mo	15.0	513	40	60
S	20.0	76	5	

of 2.5×10^{-2} of the atoms are displaced. This is about 1 displaced atom per 3 formula units. Further, about $\frac{2}{3}$ of the defects should be displaced sulfur atoms and about $\frac{1}{6}$ each displaced molybdenum and lead atoms. This low defect concentration is supported by x-ray diffraction data which appear to remain almost unchanged up to this fluence.

Assuming rigid bands, a Mo_6 octahedron surrounded by seven sulfur atoms instead of eight has 24 valence electrons. Also, complete Mo_6S_8 clusters with interstitial sulfur atoms in neighboring channels should have more than 22 valence electrons, due to the partial saturation of the electronegative sulfur atoms by the formation of sulfur-sulfur bonds. Therefore, it is conceivable that the displacement of sulfur atoms leads to a shift of the Fermi level to higher energies. Since the interaction between the Mo_6S_8 octahedra is relatively weak, the physical properties could depend strongly on the local microscopic configuration and therefore also vary locally. Near clusters with 24 valence electrons the Fermi level could be located in the gap of the density of states, thus leading to locally semiconducting behavior shunted by regions with metallic conductivity. This could explain qualitatively the observed temperature dependence of the electrical resistivity after irradiation. On the other hand, displaced atoms could enhance the interaction between the clusters leading to a reduced localization of the electrons and thus to a reduction of the peaks in $N(E)$. After high fluences (10^{15} cm^{-2}) x-ray diffraction data show a significant reduction of the intensities of the Chevrel lines indicating a highly disordered state. Smearing of $N(E)$ which then must be expected could reduce the gap in $N(E)$ and result in the observed decrease of $\rho(16 \text{ K})$.

V. CONCLUSION

Low-temperature irradiation of thin films of the Chevrel phase PbMo_6S_8 with 20-MeV sulfur ions revealed an extreme sensitivity of the superconducting properties as well as electrical resistivity to lattice defects. T_c is reduced to below 1.2 K after fluences, at least 1 order of magnitude lower than in the case of *A15* compounds or ternary rhodium borides. Simultaneously, $\rho(16 \text{ K})$ increases to almost 5 times its initial value, giving a linear T_c vs

$\rho(16 \text{ K})$ correlation. This may indicate that the same electronic band is responsible for superconductivity as well as normal-state resistivity. The T_c , critical field, and resistivity data are consistent with a defect-induced reduction of the density of states at the Fermi level. Most striking is the occurrence of a minimum in $\rho(T)$ after the very low fluence of $8 \times 10^{12} \text{ cm}^{-2}$. After about $6 \times 10^{13} \text{ cm}^{-2}$, the temperature coefficient of $\rho(T)$ is negative for $T < 290 \text{ K}$, and decreases further with irradiation, although the x-ray data show almost unchanged Chevrel line intensities in agreement with the estimated very low defect concentration of the order of 10^{-2} . From these experimental results and from a simple model for the production of lattice defects during ion irradiation, we conclude that the reason for the reduction of $N(E_F)$ is a local variation of the number of valence electrons per cluster. According to the proposed model, the most frequent type of defect should be the displacement of sulfur atoms. As outlined, both the clusters where a sulfur atom is missing as well as the clusters which are adjoining to an additional interstitial sulfur atom should have an increased number of valence electrons. Since in the case of 24 valence electrons the Chevrel phase is expected to be semiconducting, it is reasonable to relate the $\rho(T)$ behavior after irradiation to locally semiconducting regions shunted by regions with metallic conductivity. The fact that changes of the local electronic configuration by defects even at very low concentrations influence so drastically the physical properties and are not washed out by averaging over a larger range reflects the strongly localized character of the Mo *d* states. Consequently, the semiconductorlike $\rho(T)$ behavior after irradiation should be less pronounced in case of a Chevrel compound where the Mo *d* electrons are less localized, as judged from the electronic mean free path or the superconducting coherence length. This is in agreement with our results on thin films of AgMo_6S_8 which are planned to be published in detail elsewhere.

ACKNOWLEDGMENT

The authors thank Dr. E. L. Haase for part of the x-ray investigations and acknowledge financial support by the Bundesministerium für Forschung und Technologie.

- ¹R. Chevrel, M. Sergent, and J. Prigent, *J. Solid State Chem.* **3**, 515 (1971).
- ²A. Espelund, *Acta Chem. Scand.* **21**, 839 (1967).
- ³B. T. Matthias, M. Marezio, E. Corenzwit, A. S. Cooper, and H. E. Barz, *Science* **175**, 1465 (1972).
- ⁴See, e.g., *Proceedings of the International Conference on Ternary Superconductors*, edited by G. K. Shenoy, B. D. Dunlap, and F. Y. Fradin (Elsevier, New York, 1981).
- ⁵Ø. Fischer, *Appl. Phys.* **16**, 1 (1978).
- ⁶M. Marezio, P. D. Dernier, J. P. Remeika, E. Corenzwit, and B. T. Matthias, *Mater. Res. Bull.* **8**, 657 (1973).
- ⁷R. Odermatt, Ø. Fischer, H. Jones, and G. Bongi, *J. Phys. C* **7**, L13 (1974).
- ⁸S. Foner, E. J. McNiff, Jr., R. N. Shelton, R. W. McCallum, and M. B. Maple, *Phys. Lett.* **57A**, 345 (1976).
- ⁹K. Yvon, *Current Topics in Materials Science*, edited by E. Kaldis (North-Holland, Amsterdam, 1979), Vol. 3, p. 53.
- ¹⁰R. Baillif, A. Dunand, J. Müller, and K. Yvon, *Phys. Rev. Lett.* **47**, 672 (1981).
- ¹¹O. K. Andersen, W. Klose, and H. Nohl, *Phys. Rev. B* **17**, 1209 (1978); H. Nohl, W. Klose, and O. K. Andersen, in *Superconductivity in Ternary Compounds*, edited by Ø. Fischer and M. B. Maple (Springer, Berlin, 1981), Chap. 6.
- ¹²D. W. Bulet, *Phys. Rev. Lett.* **39**, 664 (1977).
- ¹³L. F. Mattheis and C. Y. Fong, *Phys. Rev. B* **15**, 1760 (1977).
- ¹⁴T. Jarlborg and A. J. Freeman, *Phys. Rev. Lett.* **44**, 178 (1980); in *Superconductivity in d- and f-Band Metals*, edited by H. Suhl and M. B. Maple (Academic, New York, 1980), p. 521.
- ¹⁵A. R. Sweedler, C. L. Snead, L. Newkirk, F. Valencia, T. H. Geballe, R. H. Schwall, B. T. Matthias, and E. Corenzwit, *Proceedings of the International Conference on Radiation Effects and Tritium Technology for Fusion Reactions*, edited by J. S. Watson and S. W. Nissen (National Technical Information Service, Springfield, Virginia, 1976), p. 422.
- ¹⁶B. S. Brown, J. W. Hafstrom, and T. E. Klippert, *J. Appl. Phys.* **48**, 1759 (1977).
- ¹⁷C. K. Banks, L. Kammerdiner, and H. L. Luo, *J. Solid State Chem.* **15**, 271 (1975).
- ¹⁸R. Flükiger, R. Baillif, and E. Walker, *Mater. Res. Bull.* **13**, 743 (1978).
- ¹⁹J. Guillevic, H. Lestrat, and D. Grandjean, *Acta Crystallogr. Sect. B* **32**, 1342 (1976).
- ²⁰H. Adrian, G. Ischenko, M. Lehmann, P. Müller, H. Braun, and G. Linker, *J. Less-Common Metals* **62**, 99 (1978).
- ²¹P. Müller, G. Ischenko, H. Adrian, J. Bieger, M. Lehmann, and E. L. Haase, in *Superconductivity in d- and f-Band Metals*, Ref. 14, p. 369.
- ²²J. M. Rowell, R. C. Dynes, and P. H. Schmidt, *Solid State Commun.* **30**, 191 (1979); R. C. Dynes, J. M. Rowell, and P. H. Schmidt, in *Proceedings of the International Conference on Ternary Superconductors*, Ref. 4, p. 169.
- ²³J. A. Woollam and S. A. Alterovitz, *J. Magn. Mater.* **11**, 177 (1979).
- ²⁴J. Bieger, H. Adrian, P. Müller, G. Saemann-Ischenko, and E. L. Haase, *Solid State Commun.* **36**, 979 (1980).
- ²⁵F. Y. Fradin, G. S. Knapp, S. D. Bader, and G. Cinader, in *Superconductivity in d- and f-Band Metals*, edited by D. H. Douglas (Plenum, New York, 1976), p. 297.
- ²⁶F. Pobell, in *Proceedings of the International Conference on Ternary Superconductors*, Ref. 4, p. 35.